Traditional Medicine Research
doi: 10.12032/TMR20201208211

Traditional Indian Medicine

Chlorogenic acid may be a potent inhibitor of dimeric SARS-CoV-2 main protease 3CLpro: an in silico study

Rajkumar Sanjay Patil[1#], Nayeem A. Khatib[1*], Vishal Shivalingappa Patil[1#*], Shailendra Sanjay Suryawanshi[2]

[1]Department of Pharmacology and Toxicology, KLE College of Pharmacy, Belagavi, KLE Academy of Higher Education and Research, JNMC Campus, Nehru Nagar, Belagavi 590010, Karnataka, India; [2]Department of Pharmaceutical Chemistry, KLE College of Pharmacy, Belagavi, KLE Academy of Higher Education and Research, JNMC Campus, Nehru Nagar, Belagavi 590010, Karnataka, India.

[#]Rajkumar Sanjay Patil and Vishal Shivalingappa Patil are co-first authors for this paper.

*Corresponding to: Nayeem A. Khatib and Vishal Shivalingappa Patil, Department of Pharmacology and Toxicology, KLE College of Pharmacy, Belagavi, KLE Academy of Higher Education and Research, JNMC Campus, Nehru Nagar, Belagavi 590010, Karnataka, India. E-mail: khatibnayeem@hotmail.com and vishalpatil6377@gmail.com.

Highlights

Chlorogenic acid, a phytocompound from traditional herb *Echinacea purpurea*, may act as a potent main protease 3CLpro inhibitor and may also inhibit the severe acute respiratory syndrome coronavirus 2 dimerization, viral gene expression, and replication within the lung epithelium.

Tradition

Echinacea purpurea, a member of the Asteraceae/Compositae family, is commonly known as purple coneflower. *E. purpurea* has a long history of medicinal use, particularly for various infections. First, in 1737, John Clayton (1686–1773) described the therapeutic use of *E. purpurea* in his *Catalogue of Plants*, *Trees*, *and Fruits Native to Virginia*, that is, "*Flora Virginica*". In 1852, *E. purpurea* was listed for the first time in *the Eclectic Dispensatory of the United States of America* for its beneficial effect against syphilis. In 1998, Thompson KD reported that Viracea (proprietary formula from Destiny BioMediX Corp), a topical microbicide, is a mixture of phytochemicals derived from *E. purpurea* and benzalkonium chloride as a potent antiviral drug against both acyclovir-resistant and acyclovir-susceptible strains of herpes simplex virus 1 and herpes simplex virus 2. The plant *E. purpurea* was also showed a significant anti-severe acute respiratory syndrome and Middle East respiratory syndrome effect.

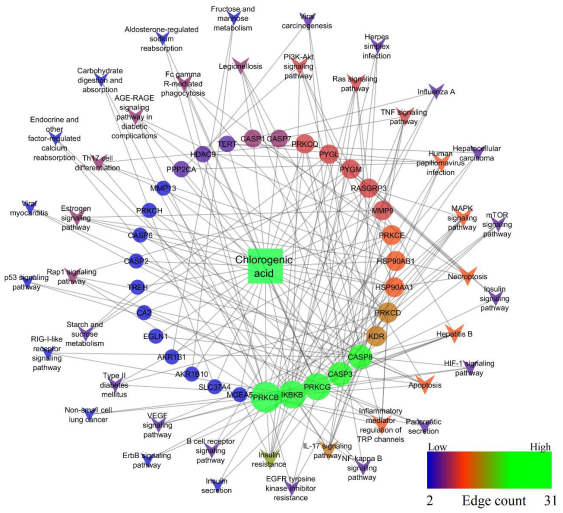

Abstract

Background: Since the emergence of coronavirus disease 2019 to date, there is no available approved drug or definitive treatment for coronavirus disease 2019 viral infection, and the identification of novel hits against therapeutic targets has become a global emergency. *Echinacea purpurea* is a traditional herb utilized to treat cough, fever, sore throat, respiratory tract infection, and so on as an immune stimulant. In this study, in silico molecular docking approach was used to screen phytocompounds from *E. purpurea* against severe acute respiratory syndrome coronavirus 2 main protease 3C-like protease (3CLpro) and severe acute respiratory syndrome coronavirus main peptidase (96% sequence similarity) to blunt the viral gene expression and viral replication. **Methods:** Initially, we screened phytocompounds for their druggability and ADMET property. Furthermore, x-ray crystallographic structures of main proteases 3CLpro and main peptidase having Protein Data Bank ID 6LU7 and 2GTB were used as protein targets for the identification of potential drug candidates. We performed docking using AutoDock Vina by PyRx 0.8 software. BIOVIA Discovery Studio Visualizer v2019 was used to analyze ligand-protein complex. The probable protein targets of the selected compound were predicted by BindingDB ($P \geq 0.7$). STRING and Kyoto Encyclopedia of Genes and Genomes pathways are utilized to identify the molecular pathways modulated by the predicted targets (FDR ≤ 0.05), and the network interaction between compounds and protein pathways was constructed by Cytoscape 3.6.1. **Results:** Among all the compounds, chlorogenic acid showed druggable characteristics and scored the lowest binding energy with main protease and main peptidase via interacting with active site 1 domain amino acid residues. Interestingly, chlorogenic acid interacted with Phe140 main protease 3CLpro, which is potentially involved in the dimerization. Enrichment analysis identified chlorogenic acid to modulate insulin resistance, necroptosis, interleukin-17, tumor necrosis factor signaling pathway, legionellosis, T helper 17 cell differentiation, advanced glycation end products and receptor for advanced glycation end products, mitogen-activated protein kinase, Ras, estrogen, vascular endothelial growth factor, B-cell receptor, nuclear factor kappa B, Rap1, hypoxia inducible factor-1, phosphatidylinositide 3-kinase-Akt, insulin, mechanistic target of rapamycin, p53, retinoic acid inducible gene I like receptor, and ErbB signaling pathways. **Conclusion:** Chlorogenic acid may act as a potent main protease 3CLpro inhibitor and may also inhibit the severe acute respiratory syndrome coronavirus 2 dimerization, viral gene expression, and replication within the lung epithelium. Chlorogenic acid may go a long way in finding one of the multipronged solutions to tackle coronavirus disease 2019 viral infection in the future.

Keywords: Molecular docking, *Echinacea purpurea*, Chlorogenic acid, COVID-19, Main protease 3CLpro, Network pharmacology

***Author contributions*:**

Rajkumar Sanjay Patil and Vishal Shivalingappa Patil performed the study, written, and drafted the manuscript; Nayeem A. Khatib supervised, revised, and finalized the manuscript; Shailendra Sanjay Suryawanshi helped Rajkumar Sanjay Patil and Vishal Shivalingappa Patil in data collection, docking studies, and manuscript writing.

***Competing interests*:**

The authors declare no conflicts of interest.

***Acknowledgments*:**

The authors are thankful to the Principal KLE College of Pharmacy, KLE Academy of Higher Education and Research, Belagavi for providing necessary infrastructure facilities.

***Abbreviations*:**

SARS-CoV, severe acute respiratory syndrome coronavirus; MERS-CoV, Middle East respiratory syndrome coronavirus; COVID-19, coronavirus disease 2019; 3CLpro, 3C-like protease; PDB, Protein Data Bank; HSV-1, herpes simplex virus 1; BBB, blood-brain barrier; HIA, human intestinal absorption; 3D, three-dimensional; DSV, Discovery Studio Visualizer; FDR, false discovery rate; IR, insulin resistance; IL-17, interleukin-17; TNF, tumor necrosis factor; AGE, advanced glycation end products; RAGE, receptor for advanced glycation end products; MAPK, mitogen-activated protein kinase; VEGF, vascular endothelial growth factor; NF-kappa B, nuclear factor kappa B; HIF-1, hypoxia inducible factor-1; PI3K, phosphatidylinositide 3-kinase; mTOR, mechanistic target of rapamycin; RIG-I-like, retinoic acid inducible gene I like; Th17, T helper 17.

***Citation*:**

Patil RS, Khatib NA, Patil VS, Suryawanshi SS. Chlorogenic acid may be a potent inhibitor of dimeric SARS-CoV-2 main protease 3CLpro: an in silico study. *Tradit Med Res*. 2021;6(2):20. doi: 10.12032/TMR20201208211.

***Executive editor*:** Rui-Wang Zhao.

***Submitted*:** 03 August 2020, ***Accepted*:** 15 November 2020, ***Online*:** 22 December 2020.

Background

Coronaviruses are a large family of viruses that belong to the Coronaviridae family. The family Coronaviridae is divided into four genera, namely, alpha, beta, gamma, and delta coronaviruses, based on the phylogenetic relationship and genomic structures [1]. It is reported that alpha and beta coronaviruses, mainly the severe acute respiratory syndrome coronavirus (SARS-CoV) and the Middle East respiratory syndrome coronavirus (MERS-CoV), transmitted to mammals, causing respiratory infections, whereas gamma and delta coronaviruses infect birds [2]. The genetic makeup of coronavirus contains accessory, structural, and nonstructural proteins. The accessory proteins perform a major role in antagonizing the host response and contribute to the pathogenesis of coronavirus disease 2019 (COVID-19) [3]. The coronavirus genome encodes four major structural proteins, namely, the spike (S) protein, nucleocapsid (N) protein, membrane (M) protein, and the envelope (E) protein, all of which are required to produce a complete structural morphology of viral particles [4, 5].

2019-nCoV is a new strain of coronavirus identified at the end of 2019 in Wuhan, China, and on 30 January 2020, the outbreak in China was declared by the Emergency Committee of the WHO [6]. COVID-19 has become an important public issue across the world. A total of about 74,000,000 confirmed cases and 1,650,000 deaths have been reported in 210 countries and territories from COVID-19 till 17 Dec 2020 [7]. The virus mainly attacks the respiratory tract and causes many symptoms such as fever, dyspnea, and bilateral lung infiltration, which are similar to those of the previously reported SARS-CoV and the MERS-CoV infection [8].

After the analysis of different therapeutic targets of coronavirus, three important known proteins of coronavirus, including papain-like protease, 3C-like protease (3CLpro), and spike protein, were discovered, which are become attractive targets for investigation of new potential antiviral agents [9]. It is reported that the spike protein of both SARS-CoV-2 and SARS-CoV binds to angiotensin-converting enzyme 2 receptor with high affinity and enters into host cells to exert its pathogenicity [10]. Recently, Liu et al. in January 2020 have successfully crystallized the main protease 3CLpro as a potential therapeutic target from COVID-19 and it has been structured and deposited in the Protein Data Bank (PDB) [11]. COVID-19 main protease shares 96% sequence similarity with SARS coronavirus main peptidase [12]. SARS-CoV-2 main protease 3CLpro and SARS main peptidase are key proteins involved in viral translation, replication, and life cycle of the virus in human host cells.

Therefore, researchers are focusing on both the main protease and main peptidase to develop a potential antiviral treatment. Compounds targeting these proteins could blunt the function of viral pathogenesis [13]. Numerous researchers performed virtual screening of phytocompounds to identify the small molecule, which can inhibit the main protease function [14–17] and suggested some broad-spectrum antiviral drugs such as human immunodeficiency virus proteases, neuraminidase inhibitors, and nucleoside analogs as a promising treatment for COVID-19. Antimalarial drugs, for example, chloroquine, hydroxychloroquine, and some antiviral drugs like oseltamivir, nelfinavir, lopinavir, ganciclovir, remdesivir, ritonavir, and so on are clinically tested against COVID-19 infection and currently utilized as prophylaxis [18]. However, there is no Food and Drug Administration approved or specific treatment that has been developed to combat COVID-19. Hence, considering the risk factors associated with a viral infection, the identification of a specific drug molecule to target COVID-19 infection becomes a global emergency. Traditional medicinal plants have been in use since ancient times and have the potency to treat infectious diseases [19].

Echinacea purpurea, a member of the Asteraceae/Compositae family [20], is commonly known as purple coneflower [20, 21]. *E. purpurea* has a long history of medicinal use, particularly for various infections. First, in 1737, John Clayton (1686–1773) described the therapeutic use of *E. purpurea* in his *Catalogue of Plants*, *Trees*, *and Fruits Native to Virginia*, that is, "*Flora Virginica*" [22, 23]. In 1852, *E. purpurea* was listed for the first time in *the Eclectic Dispensatory of the United States of America* for its beneficial effect against syphilis [22, 23]. Furthermore, in 1994, a clinical trial by D Melchart reported *E. purpurea* as an immunomodulator [24]. In 1998, Thompson KD reported that Viracea (proprietary formula from Destiny BioMediX Corp), a topical microbicide, is a mixture of phytochemicals derived from *E. purpurea* and benzalkonium chloride as a potent antiviral against both acyclovir-resistant and acyclovir-susceptible strains of herpes simplex virus 1 (HSV-1) and HSV-2 virus [25]. Native Americans used the plant for enhancing the human immune system [20, 21]. The plant was not approved by the US Food and Drug Administration for its therapeutic use but it was adopted by central US settlers in the 1800s [26]. The plant is rich in phenolic compounds (caffeic acid derivatives), alkamide derivatives, and other phytocompounds and possesses antifungal [27], anti-inflammatory [29], antioxidant [30], and other activities. The plant *E. purpurea* was also tested for its in vitro activity against SARS and MERS and showed a significant anti-SARS and MERS effect [31].

In this study, we screened phytocompounds, mainly caffeic acid, caftaric acid, chlorogenic acid, ferulic acid, gallic acid, and 4-hydroxy benzoic acid, from *E.*

purpurea against COVID-19 main protease and SARS-CoV main peptidase using molecular docking study. We identified chlorogenic acid potent lead molecule against SARS-CoV-2 main protease 3CLpro and SARS main peptidase.

Materials and methods

Drug-likeness property of bioactive phytocompounds

Molinspiration (https://www.molinspiration.com/cgi-bin/properties) and MolSoft (https://molsoft.com/mprop/) web servers were used to predict the drug-likeness properties of phytocompounds. Drug-like properties were calculated based on Lipinski's rule of five, which proposes that molecules should possess molecular weight ≤ 500, C logP ≤ 5, less than 10 hydrogen bonds acceptor, and less than 5 hydrogen bond donors [32]. The canonical simplified molecular line-entry systems were retrieved from PubChem and submitted as input to Molinspiration and MolSoft web server to predict drug-like properties of compounds [33].

Pharmacokinetics and toxicity predictions

In the drug development process, the pharmacokinetic properties such as absorption, distribution, metabolism, and excretion and toxicity studies of ligand molecules play an important role. Hence, we used the online server PreADMET (http://preadmet.bmdrc.org) to predict several pharmacokinetics and toxicological parameters. PreADMET calculates pharmacokinetic and toxicological properties such as blood-brain barrier (BBB), buffer solubility, human intestinal absorption (HIA), P-glycoprotein, skin permeability, plasma protein binding, and carcinogenic and mutagenic effects [34].

Preparation of ligand

The three-dimensional (3D) structures of all ligand molecules were retrieved from the PubChem chemical database (https://pubchem.ncbi.nlm.nih.gov/) in structural data format and converted to PDB format using Discovery Studio Visualizer (DSV) 2019. PubChem is a universal database that stores chemical structural information, including their biological activities. Furthermore, we minimized ligands' free energy using the MMFF94 force field using Marvin Sketch software to remove the clashes within the atoms [35].

Preparation of target protein

We obtained the 3D x-ray crystallographic structures of both targets COVID-19 main protease 3CLpro (PDB ID: 6LU7) and SARS-CoV main peptidase (PDB ID: 2GTB) from PDB (www.rcsb.org). 6LU7 has two chains, "A and C". Chain A contains SARS-CoV-2 main protease enzyme and chain C is a native ligand of protein (mainly, a peptide designed to inhibit the main protease). 2GTB has three chains. Chain A contains SARS coronavirus main peptidase (3CLpro) and the other two chains are native ligands of the protein. Hence, we used chain A of both proteins for the preparation of the macromolecule. Furthermore, we cleaned the binding pocket by removing water molecules and heteroatoms using the DSV 2019 to eliminate the docking interferences; this makes calculations easier so that ligand can form satisfactory interactions with the protein molecule.

Ligand-protein docking study

For molecular docking, we used AutoDock Vina by PyRx 0.8. The target and ligands PDB files were loaded into PyRx software, and AutoDock Vina preferences were obtained for both ligand and target in PDBQT format. The grid box was generated to the active site, and the exhaustiveness was set to 100. After completion of the docking algorithm, the ligand-protein complexes that have the best conformation and lowest binding energy were selected and visualized in DSV 2019 for their conventional and hydrophobic interactions. Furthermore, the change in the ligand orientation pre- and postdocking simulation was observed in the steric and electrostatic properties.

Target prediction and gene set enrichment analysis

BindingDB and SwissTargetPrediction online server were used to predict probable protein targets of the selected compound at a probability score of ≥ 0.7 and ≥ 0.09, respectively. To retrieve the gene ID of predicted protein targets, the UniProt database (https://www.uniprot.org/) was used [36]. To analyze the protein-protein interaction with the species limited to "*Homo sapiens*", the set of proteins were submitted as input to the search tool for the Retrieval of Interacting Genes/Proteins database STRING v.11.0 (https://string-db.org/), and Kyoto Encyclopedia of Genes and Genomes database was utilized to identify the molecular pathways modulated by chlorogenic acid predicted targets at the false discovery rate (FDR) cut-off value of ≤ 0.05 [37].

Network analysis

Based on the enrichment analysis, protein targets involving pathways of COVID-19 and other viral infections, inflammation, immune system, and complex polygenic disorders such as metabolic syndromes, namely, diabetes mellitus, hypertension, and cardiac failure are selected. The datasheet was built for the interaction between chlorogenic acid, selected protein targets, and pathways, and the network between them was constructed using Cytoscape 3.6.1 software. The network is treated as directed by using the command "network analyzer", and the topological parameter "edge count" was applied to identify the connections' degree among the nodes (blue color

doi: 10.12032/TMR20201208211

represents low edge count, and green color represents high edge count) [38, 39]. The square shape represents the compound, the round shape represents probable protein molecules targeted by the compound, and the down arrow represents modulated molecular pathways by protein molecules targeted by the compound.

Results

Drug-likeness property of bioactive phytocompounds

MolSoft online server was used to screen the phytocompounds' druggable characteristics. Among the selected compounds, only chlorogenic acid showed potent drug-like properties. The drug-likeness score of chlorogenic acid was found to be 0.72. Furthermore, chlorogenic acid was classified under the small molecules based on Lipinski's rule of five because chlorogenic acid MW is 354.31 (< 500) and hydrogen bond donor and hydrogen bond acceptor were 6 and 9, respectively. LogP value is 1.61. Herein, chlorogenic acid obeyed the rule of five and showed positive druggable characteristics. Similarly, other compounds obeyed Lipinski's rule of five but did not show a positive drug-likeness score. The drug-likeness property of each compound was shown in Table 1.

Pharmacokinetics and toxicity predictions

The PreADMET server was used to predict ADMET profile of phytocompounds. Caffeic acid, ferulic acid, gallic acid, and 4-hydroxy benzoic acid were predicted to cross BBB. However, caftaric acid and chlorogenic acid were predicted to cross BBB poorly. HIA of caffeic acid, ferulic acid, gallic acid, and 4-hydroxy benzoic acid was found between 50% and 90%, whereas chlorogenic acid and caftaric acid were found to be 30.42% and 18.28%, respectively. All the compounds were predicted to be an inhibitor of CYP2C9 and predicted to be a mutagen. Except for caftaric acid and chlorogenic acid, all the drugs showed the noncarcinogenic property in mice, whereas chlorogenic acid and 4-hydroxy benzoic acid were predicted for their noncarcinogenic effect in rats. Table 1 shows the overall ADMET profile of each compound.

Table 1 Druggability, pharmacokinetic, and toxicity profile of phytocompounds

Compounds	Caffeic acid	Caftaric acid	Chlorogenic acid	Ferulic acid	Gallic acid	4-Hydroxy benzoic acid
Mol formula	$C_9H_8O_4$	$C_{13}H_{12}O_9$	$C_{16}H_{18}O_9$	$C_{10}H_{10}O_4$	$C_7H_6O_5$	$C_7H_6O_3$
Mol weight (g/mol)	180.16	312.23	354.31	194.18	170.12	138.12
LogP	1.27	−0.85	−0.20	1.61	0.78	1.43
HBD	3	5	6	2	4	2
HBA	4	9	9	4	5	3
TPSA	77.75	161.59	164.74	66.76	97.98	57.53
DLS	−0.35	−0.02	0.79	−0.61	−0.22	−0.37
BBB (logBB)	0.50	0.03	0.03	0.76	0.64	0.35
BS (mg/L)	2.00E+05	3.40E+06	8.17E+05	8.13E+04	5.98E+04	1.56E+06
$CaCO_2p$ (nm/sec)	21.11	14.34	18.72	21.12	20.31	13.85
CYP2C19	Non	Inhibitor	Inhibitor	Non	Inhibitor	Inhibitor
CYP2C9	Inhibitor	Inhibitor	Inhibitor	Inhibitor	Inhibitor	Inhibitor
CYP2D6	Non	Non	Non	Non	Non	Non
CYP3A4	Inhibitor	Inhibitor	Inhibitor	Non	Non	Inhibitor
HIA (%)	82.30	18.28	30.43	90.60	88.14	53.70
P-gp	Non	Non	Non	Non	Non	Non

Table 1 Druggability, pharmacokinetic, and toxicity profile of phytocompounds (*Continued*)

Compounds	Caffeic acid	Caftaric acid	Chlorogenic acid	Ferulic acid	Gallic acid	4-Hydroxy benzoic acid
PPB (%)	40.29	53.66	41.96	50.41	8.041	65.38
Water solubility (mg/L)	4878.52	3883.01	7919.12	2387.53	19482.50	72333.40
SP (logKp, cm/h)	−2.67	−3.86	−3.89	−1.87	−2.23	−3.63
Ames test	Mutagen	Mutagen	Mutagen	Mutagen	Mutagen	Mutagen
Carcinogenicity (mouse)	Negative	Positive	Positive	Negative	Negative	Negative
Carcinogenicity (rat)	Positive	Positive	Negative	Positive	Positive	Negative
hERG inhibition	Medium risk	Medium risk	Medium risk	Medium risk	Low risk	Low risk
FAT (Medika)	0.23	0.65	2.64	0.20	0.59	0.51
FAT (Minnow)	0.11	0.49	2.20	0.13	0.23	0.18

HBD, hydrogen bond donor; HBA, hydrogen bond acceptor; TPSA, topological polar surface area; DLS, drug-likeness score; BBB, blood-brain barrier; BS, buffer solubility; $CaCO_2p$ = $CaCO_2$ permeability: the predicted value of intestinal absorption through $CaCO_2p$; HIA, human intestinal permeability; P-gp, P-glycoprotein; SP, skin permeability; PPB, plasma protein binding; hERG inhibition, the predicted result of hERG (the human e*ther-à-go-go*-related gene) inhibition by compounds; FAT, fish aqueous toxicity.

Characteristics of protein molecules

PROCHECK and ERRAT online servers were used to identify the amino acid distribution and to predict the quality of the x-ray crystallographic protein molecules used in this study. About 90.6% of amino acid residues of main protease 6LU7 were present in the most favored region and about 8.7% were in the additional allowed region. However, only one amino acid, Asn84, was present in the disallowed region. Similarly, about 90% of amino acid residues of main peptidase (2GTB) were present in the most favored region and 8.1% were in the additional allowed region. However, only three amino acids, Asn84, Tyr154, and ILE286, were present in the disallowed region. The overall quality of 6LU7 and 2GTB was found to be 96.55% and 95.4%, respectively. Phe140, Gly143, His163, His164, Glu166, Gln189, and Thr190 are the active site amino acid residues present in the main protein. Similarly, Thr25, His41, Met49, Tyr54, Phe140, Leu141, Asn142, Gly143, Ser144, Cys145, His163, His164, Met165, Glu166, Leu167, Pro168, His172, Asp198, Arg188, Gln189, Gln192, Ala193, Lys236, Tyr237, and Gln273 are the active site amino acid residues present in the main peptidase.

Ligand-protein docking study

AutoDock by PyRx 0.8v was used to perform a molecular docking study to identify the probable binding affinity and molecular interactions of phytocompounds with COVID-19 main protease and SARS main peptidase. Among all the compounds, caftaric acid and chlorogenic acid showed the highest binding affinity with main protease, that is, −6.0 kcal/mol, and formed 5 and 4 hydrogen bond interactions with active site amino acid residues, respectively. Among them, caftaric acid formed 2 bonds with active site residues, Gly143 and Thr190, whereas chlorogenic acid formed 3 bonds, Phe140, Glu166, and Thr190, which indicates the highest affinity of chlorogenic acid toward the main protease. Furthermore, the distance between the active site residue and chlorogenic acid functional groups was identified as Phe140…OH (2.77Å), Glu166…OH (2.33Å), and Thr190…OH (2.10Å). Similarly, among all the compounds, chlorogenic acid showed the highest binding affinity with main peptidase (−7.4 kcal/mol) and formed two hydrogen bond interactions with active site amino acid residues, that is, His41 and His163. Interestingly, none of the compounds showed hydrogen bond interaction with the active site residues, except for chlorogenic acid (Table 2). Furthermore, the percentage change in orientation of chlorogenic acid with main protease 3CLpro pre- and postdocking in the steric property was found to be 18.44% and at electrostatic was 44.50%. Similarly, chlorogenic acid with main peptidase in the steric property was found to be 17.71% and at electrostatic was 29.86%. The affinity and orientation of chlorogenic acid main protease 3CLpro and main peptidase are shown in Figure 1 and Figure 2.

doi: 10.12032/TMR20201208211

Table 2 Binding affinity and hydrogen bond interactions of phytocompounds with 6LU7 and 2GTB

Compounds	PubChem ID	Binding energy (kcal/mol)		Hydrogen bond interactions	
		6LU7	2GTB	Amino acids of 6LU7 involved in the interaction	Amino acids of 2GTB involved in the interaction
Caffeic acid	689043	−5.4	−6.6	HIS A:41, PHE140 A:140, and GLU A:166	GLN A:110, THR A:111, ASN A:151, PRO A:293, PHE A:294, ASP A:295, and ARG A:298
Caftaric acid	6440397	−6.0	−7.1	LEU A:141, GLY A:143, CYS A:145, MET A:165, and THR A:190	THR A:111, LEU A:202, THR A:292, and ARG A:298
Chlorogenic acid	1794427	−6.0	−7.4	PHE A:140, LEU A:141, GLU A:166, and THR A:190	HIS A:41 and HIS A:163
Ferulic acid	445858	−5.3	−5.9	Nil	VAL A:104, GLN A:110, THR A:111, and ASP A:295
Gallic acid	370	−5.1	−6.0	SER A:144 and GLU A:166	TRP A:218
4-Hydroxy benzoic acid	135	−4.5	−5.7	GLU A:166	PHE A:219, LEU A:271, and TRP A:218

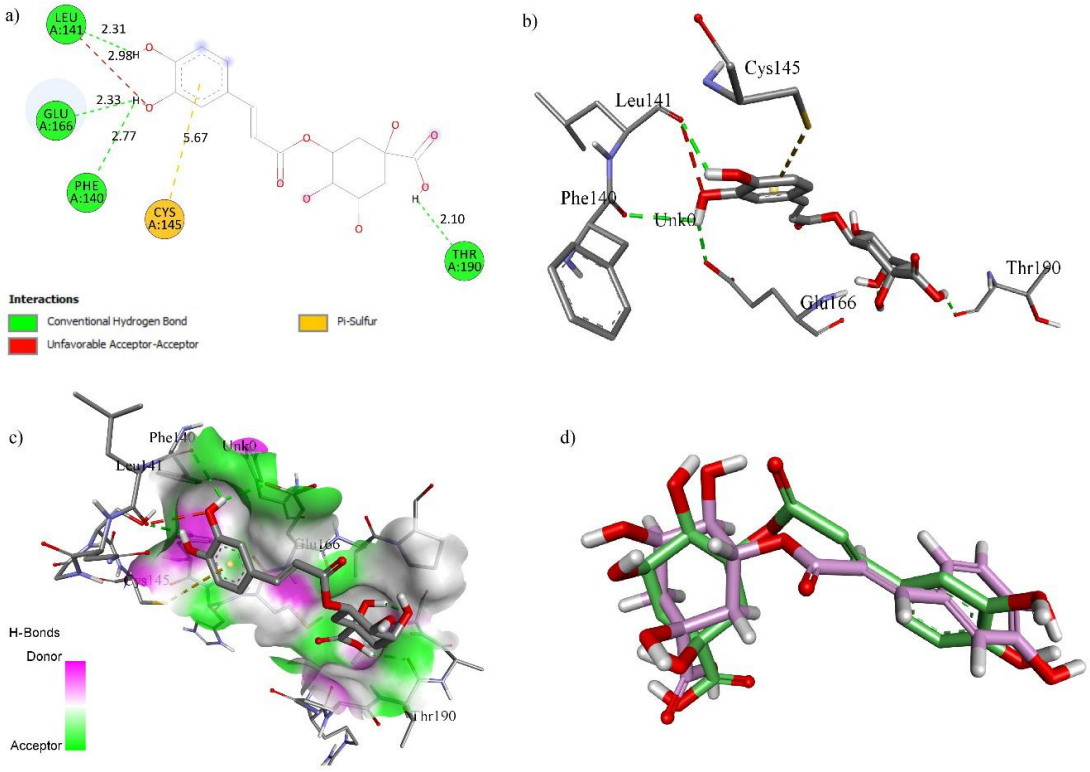

Figure 1 Interaction of chlorogenic acid with main protease 3CLpro. a) Distance between chlorogenic acid functional group and main protease 3CLpro. b) 3D representation. c) Chlorogenic acid within main protease 3CLpro binding pocket. d) Orientation of chlorogenic acid before and after docking simulation. 3CLpro, 3C-like protease; 3D, three-dimensional.

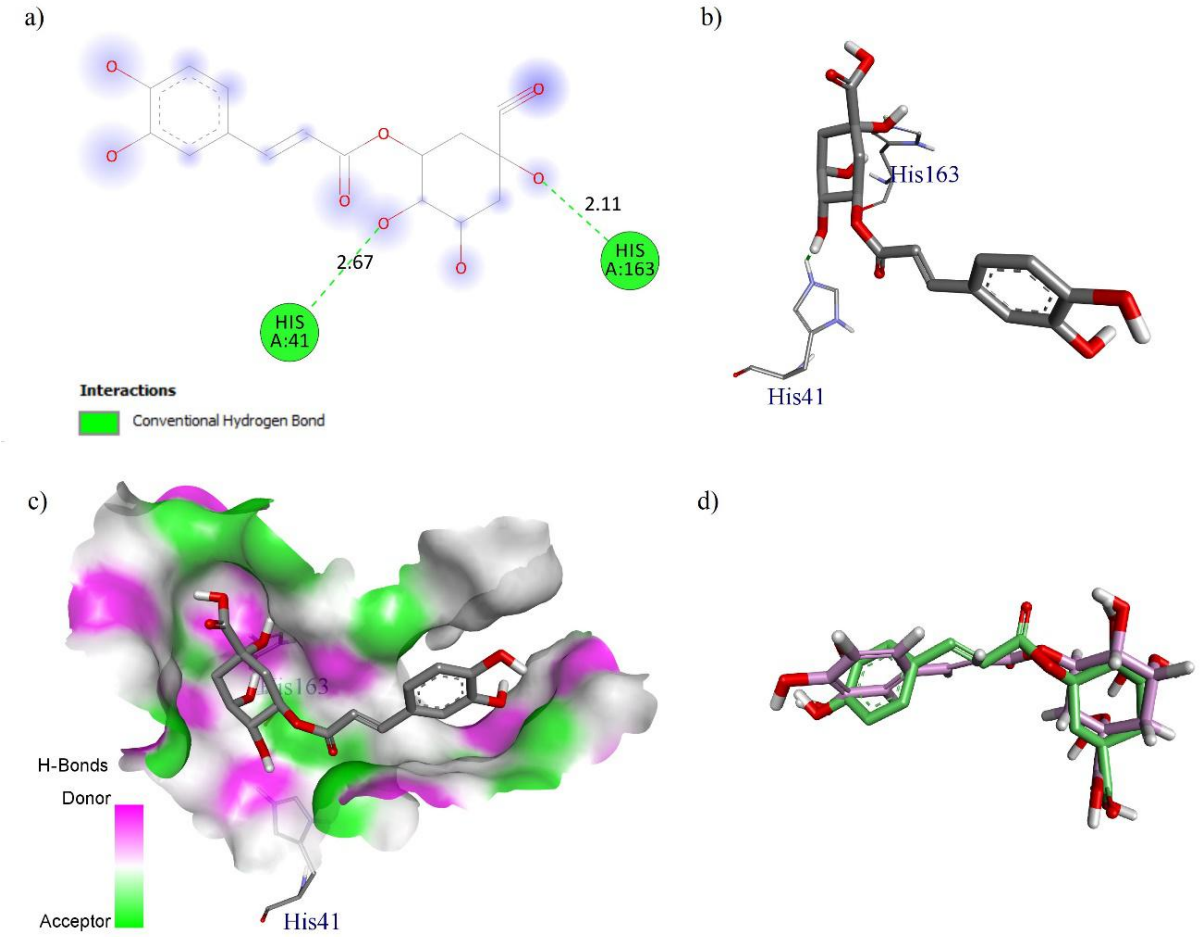

Figure 2 Interaction of chlorogenic acid with SARS-CoV main peptidase. a) Distance between chlorogenic acid functional group and main peptidase. b) 3D representation. c) Chlorogenic acid within main peptidase binding pocket. d) Orientation of chlorogenic acid before and after docking simulation. SARS-CoV, severe acute respiratory syndrome coronavirus; 3D, three-dimensional.

Target prediction, gene set enrichment, and network analysis

A total of 27 probable protein targets were identified from BindingDB ($P \geq 0.7$) and 36 from SwissTargetPrediction ($P \geq 0.09$). The gene set enrichment analysis of predicted targets identified 31 protein targets to modulate 92 molecular pathways. Among them, 41 molecular pathways were potentially involved in COVID-19 and other viral infections, inflammation, immune system, and complex polygenic disorders such as metabolic syndromes, namely, diabetes mellitus, hypertension, and cardiac failure. Insulin resistance (IR) scored the lowest FDR value of 1.73E-07 and scored the highest edge count within the network via modulating 8 protein targets, namely, PYGM, PYGL, PRKCQ, PRKCB, PRKCE, MGEA5, PRKCD, and IKBKB. Following the IR, intracellular signaling pathways such as interleukin-17 (IL-17), tumor necrosis factor (TNF), advanced glycation end products (AGE) and receptor for advanced glycation end products (RAGE), mitogen-activated protein kinase (MAPK), Ras, estrogen, vascular endothelial growth factor (VEGF), B-cell receptor, nuclear factor kappa B (NF-kappa B), Rap1, hypoxia inducible factor-1 (HIF-1), phosphatidylinositide 3-kinase (PI3K)-Akt, insulin, mechanistic target of rapamycin (mTOR), p53, retinoic acid inducible gene I like (RIG-I-like) receptor, ErbB signaling pathways and necroptosis, legionellosis, and T helper 17 (Th17) cell differentiation were identified to be the next highly enriched molecular pathways with < 0.05 FDR value (Table 3). Figure 3 presents the network representation of chlorogenic acid, protein targets, and pathways.

Discussion

The ecological environmental changes and the variations in the pathogens have led to a surge in the number of new emerging infectious diseases. The current pandemic COVID-19 infection is responsible

doi: 10.12032/TMR20201208211

for a large number of deaths worldwide and becomes a public health challenge. To date, many researchers made several attempts to identify novel antiviral agents, focusing on the development of novel vaccines, but none of the antiviral compounds showed a significant effect against SARS-CoV-2. Recently, Hydroxychloroquine and Chloroquine were utilized as prophylaxis but these agents are causing negative effects on patients with diabetes, hypertension, and heart disease. However, traditional medicines have broad prospects for the treatment of infectious diseases since ancient times. In 2002, about 58.3% of SARS confirmed patients received traditional Chinese herbal medicine and the symptoms associated with SARS such as fever, cough, and dyspnea significantly improved, improving absorption of pulmonary infiltration and quality of life.

In our study, *E. purpurea*, a member of the Echinacea family, was used to screen against COVID-19 infection. *E. purpurea* is a well-known antiviral herb, and traditionally, it is used to treat the common cold, coughs, bronchitis, urinary tract infections, upper respiratory tract infection, and inflammatory conditions [22, 23]. *E. purpurea* is reported for its immunostimulant [28] and anti-inflammatory activities [29]. The beneficial effect of *E. purpurea* against respiratory infection was documented via preclinical and clinical studies. Herein, seven bioactive phytocompounds were identified to screen their affinity toward SARS-CoV-2 main protease and SARS-CoV main peptidase. The results revealed that chlorogenic acid has a positive drug-like property and is predicted to have the highest binding affinity with active site residues, that is, Phe140, Glu166, and Thr190 of SARS-CoV-2 main protease and His41 and His163 of SARS-CoV main peptidase. Importantly, SARS-CoV-2 main protease is active in a dimeric form and plays a key role in polyprotein processing, and dimerization is important for catalytic activity. In SARS-CoV-2 main protease, Phe140 is potentially involved in dimerization. In this study, chlorogenic acid showed hydrogen bond interaction with Phe140 dimerization residue.

Table 3 Molecular pathway enrichment analysis of protein targets modulated by chlorogenic acid

Pathway name	Gene count	FDR	Set of genes within the pathway
IR	8	1.73E−07	PYGM, PYGL, PRKCQ, PRKCB, PRKCE, MGEA5, PRKCD, IKBKB
IL-17 signaling pathway	7	8.32E−07	MMP13, CASP3, HSP90AA1, CASP8, HSP90AB1, MMP9, IKBKB
Inflammatory mediator regulation of transient receptor potential channels	6	1.22E−05	PRKCQ, PRKCG, PRKCB, PRKCE, PRKCH, PRKCD
Apoptosis	6	8.00E−05	CASP6, CASP3, CASP2, CASP8, CASP7, IKBKB
Hepatitis B	6	9.51E−05	PRKCG, PRKCB, CASP3, CASP8, MMP9, IKBKB
Necroptosis	6	1.40E−04	PYGM, PYGL, HSP90AA1, CASP8, HSP90AB1, CASP1
TNF signaling pathway	5	3.00E−04	CASP3, CASP8, CASP7, MMP9, IKBKB
Legionellosis	4	3.40E−04	CASP3, CASP8, CASP7, CASP1
Starch and sucrose metabolism	3	1.70E−03	PYGM, PYGL, TREH
Fc gamma R-mediated phagocytosis	4	1.70E−03	PRKCG, PRKCB, PRKCE, PRKCD
AGE-RAGE signaling pathway in diabetic complications	4	2.00E−03	PRKCB, PRKCE, CASP3, PRKCD
MAPK signaling pathway	6	2.10E−03	PRKCG, KDR, PRKCB, CASP3, RASGRP3, IKBKB
Th17 cell differentiation	4	2.10E−03	PRKCQ, HSP90AA1, HSP90AB1, IKBKB
Type II diabetes mellitus	3	2.60E−03	PRKCE, PRKCD, IKBKB
Human papillomavirus infection	6	2.60E−03	TERT, CASP3, CASP8, HDAC9, PPP2CA, IKBKB
IR	8	1.73E−07	PYGM, PYGL, PRKCQ, PRKCB, PRKCE, MGEA5, PRKCD, IKBKB

Table 3 Molecular pathway enrichment analysis of protein targets modulated by chlorogenic acid (*Continued*)

Pathway name	Gene count	FDR	Set of genes within the pathway
Ras signaling pathway	5	3.70E−03	PRKCG, KDR, PRKCB, RASGRP3, IKBKB
Estrogen signaling pathway	4	4.10E−03	HSP90AA1, HSP90AB1, MMP9, PRKCD
VEGF signaling pathway	3	4.40E−03	PRKCG, KDR, PRKCB
B-cell receptor signaling pathway	3	6.50E−03	PRKCB, RASGRP3, IKBKB
Epidermal growth factor receptor tyrosine kinase inhibitor resistance	3	7.80E−03	PRKCG, KDR, PRKCB
NF-kappa B signaling pathway	3	1.18E−02	PRKCQ, PRKCB, IKBKB
Pancreatic secretion	3	1.18E−02	PRKCG, CA2, PRKCB
Rap1 signaling pathway	4	1.22E−02	PRKCG, KDR, PRKCB, RASGRP3
HIF-1 signaling pathway	3	1.22E−02	PRKCG, PRKCB, EGLN1
PI3K-Akt signaling pathway	5	1.40E−02	KDR, HSP90AA1, HSP90AB1, PPP2CA, IKBKB
Fructose and mannose metabolism	2	1.52E−02	AKR1B1, AKR1B10
Aldosterone-regulated sodium reabsorption	2	1.75E−02	PRKCG, PRKCB
Carbohydrate digestion and absorption	2	2.07E−02	PRKCB, SLC37A4
Insulin signaling pathway	3	2.16E−02	PYGM, PYGL, IKBKB
Endocrine and other types of factor-regulated calcium reabsorption	2	2.46E−02	PRKCG, PRKCB
mTOR signaling pathway	3	2.72E−02	PRKCG, PRKCB, IKBKB
Viral myocarditis	2	3.20E−02	CASP3, CASP8
Hepatocellular carcinoma	3	3.32E−02	PRKCG, PRKCB, TERT
Influenza A	3	3.54E−02	PRKCB, IKBKB, CASP1
p53 signaling pathway	2	3.87E−02	CASP3, CASP8
RIG-I-like receptor signaling pathway	2	3.87E−02	CASP8, IKBKB
Herpes simplex infection	3	3.87E−02	CASP3, CASP8, IKBKB
Viral carcinogenesis	3	3.87E−02	CASP3, CASP8, HDAC9
Non-small-cell lung cancer	2	3.87E−02	PRKCG, PRKCB
ErbB signaling pathway	2	4.90E−02	PRKCG, PRKCB
Insulin secretion	2	4.96E−02	PRKCG, PRKCB

IR, insulin resistance; FDR, false discovery rate; IL-17, interleukin-17; TNF, tumor necrosis factor; AGE, advanced glycation end products; RAGE, receptor for advanced glycation end products; MAPK, mitogen-activated protein kinase; Th17, T helper 17; VEGF, vascular endothelial growth factor; NF-kappa B, nuclear factor kappa B; HIF-1, hypoxia inducible factor-1; PI3K, phosphatidylinositide 3-kinase; mTOR, mechanistic target of rapamycin; RIG-I-like, retinoic acid inducible gene I like.

doi: 10.12032/TMR20201208211

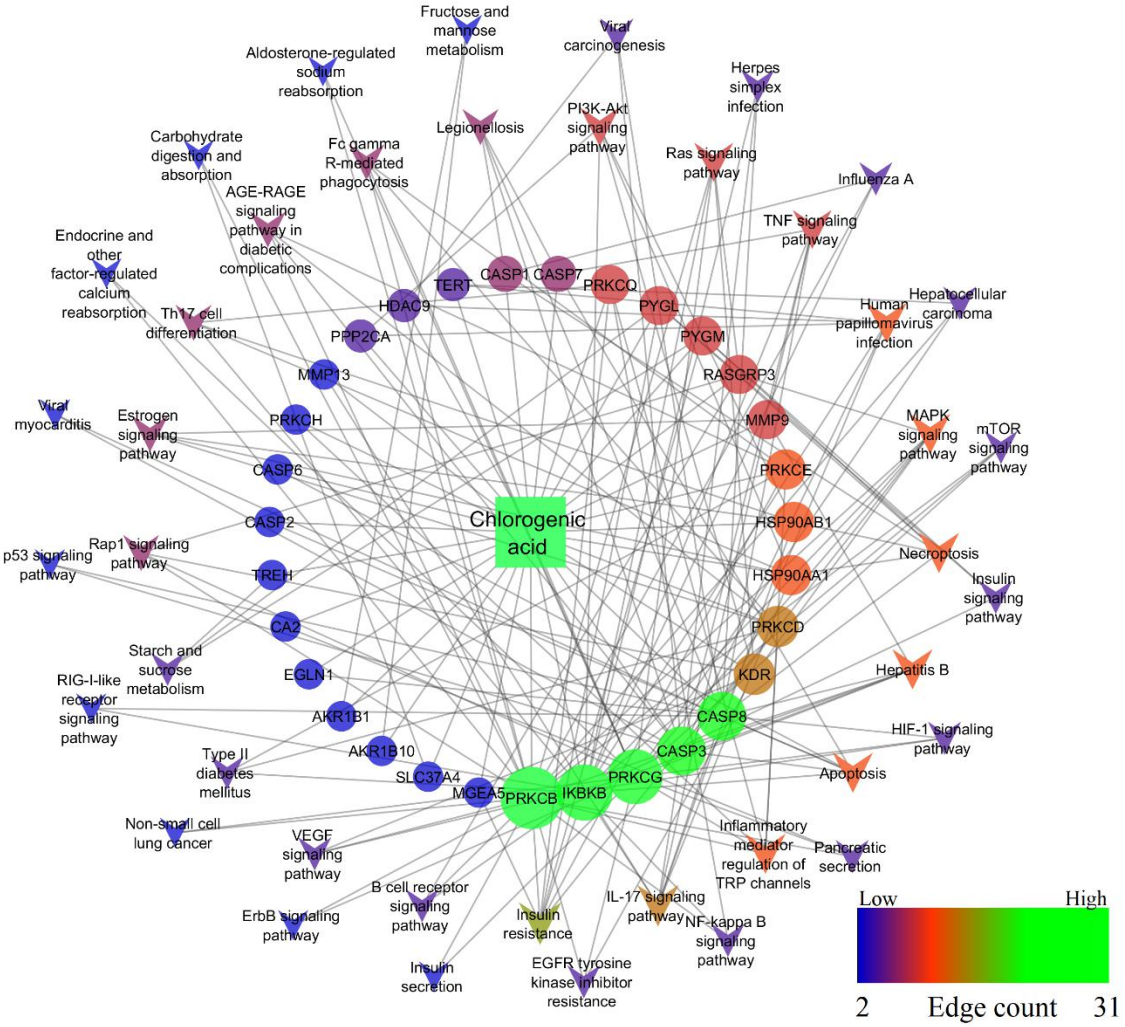

Figure 3 Network representation of chlorogenic acid, protein targets, and molecular pathways. The square shape represents compound, the round shape represents probable protein targets, and the down arrow represents modulated molecular pathways. IL-17, interleukin-17; TNF, tumor necrosis factor; AGE, advanced glycation end products; RAGE, receptor for advanced glycation end products; MAPK, mitogen-activated protein kinase; VEGF, vascular endothelial growth factor; NF-kappa B, nuclear factor kappa B; HIF-1, hypoxia inducible factor-1; PI3K, phosphatidylinositide 3-kinase; mTOR, mechanistic target of rapamycin; RIG-I-like, retinoic acid inducible gene I like; Th17, T helper 17.

In the previous studies, chlorogenic acid was reported as a potent anti-inflammatory, analgesic, antipyretic, antiviral, and immunomodulatory agent. Chlorogenic acid reduced the inflammation caused by a viral infection and showed potent antiviral efficacy against many viruses such as HSVs [41, 42], hepatitis B virus [43], human immunodeficiency virus [44, 45], adenovirus [43], and HSV-1 virus [46]. Chlorogenic acid is used for viral upper respiratory tract infection caused by the influenza virus, parainfluenza virus, and respiratory syncytial virus [47]. Molecular docking analysis of chlorogenic acid revealed inhibitory potential against neuraminidase of influenza viruses H1N1 [48], H5N1 [49], and H7N9 [50]. Chlorogenic acid has been found to exert antiviral effects on the influenza virus by inhibiting neuraminidase enzyme. Chlorogenic acid showed a high binding affinity with the enzyme "neuraminidase" and was found to be a potent inhibitor for neuraminidase of H7N9, which might be effective for inhibition of replication [51]. Furthermore, the literature showed chlorogenic acid as a potent anti-inflammatory agent that inhibits the secretion of inflammatory mediators such as interleukin-6 and TNF-α induced by influenza virus infection and found to alleviate inflammation and damage in lung tissues [52].

Based on the antiviral, anti-inflammatory, analgesic, antidiabetic, antipyretic, and immunomodulatory reports on chlorogenic acid, we further aimed in this study to identify potential protein targets and

molecular pathways modulated by the chlorogenic acid utilizing experimentally determined protein-ligand interaction database, that is, BindingDB through gene set pathway enrichment and network pharmacology approaches. The enrichment analysis identified IR as a highly enriched pathway and it was found to score the highest edge count within the network. Following the IR pathway, necroptosis, legionellosis, Th17 cell differentiation, IL-17, TNF, AGE-RAGE, MAPK, Ras, estrogen, VEGF, B-cell receptor, NF-kappa B, Rap1, HIF-1, PI3K-Akt, insulin, mTOR, p53, RIG-I-like receptor, and ErbB signaling pathways were identified to be the next highly enriched molecular pathways by chlorogenic acid. Chlorogenic acid predicted protein targets were found to be involved in the inflammatory mediator regulation of transient receptor potential channels, apoptosis, hepatitis B, starch and sucrose metabolism, Fc gamma R-mediated phagocytosis, human papillomavirus infection, pancreatic secretion, hepatocellular carcinoma, influenza A, herpes simplex infection, viral carcinogenesis, non-small-cell lung cancer, and insulin secretion. Hence, the previous studies and the current study findings strongly support the beneficial effects of chlorogenic acid as a potent antiviral lead molecule against newly emerged COVID-19 infection, inflammation, immune system, and complex polygenic disorders such as metabolic syndromes, namely, diabetes mellitus, hypertension, cardiac failure, stroke, and so on.

Conclusion

This study suggests that chlorogenic acid targets the dimerization of SARS-CoV-2 main protease and displays broad-spectrum antiviral activity by preventing the replication and proliferation of the SARS-CoV-2 and via targeting the multiprotein molecules, namely, PRKCB, IKBKR, PRKCG, CASP3, CASP8, KDR, and so on, and modulating molecular pathways such as IL-17, TNF, AGE-RAGE, MAPK, Ras, estrogen, VEGF, B-cell receptor, NF-kappa B, Rap1, HIF-1, PI3K-Akt, insulin, mTOR, p53, RIG-I-like receptor, and ErbB signaling pathways involved in the disease pathogenesis.

References

1. Cui J, Li F, Shi ZL. Origin and evolution of pathogenic coronaviruses. *Nat Rev Microbiol*. 2019;17(3):181–192.
2. Banerjee A, Kulcsar K, Misra V, Frieman M, Mossman K. Bats, and coronaviruses. *Viruses*. 2019;11(1):41.
3. Narayanan K, Huang C, Makino S. SARS coronavirus accessory proteins. *Virus Res*. 2008;133(1):113–121.
4. Masters PS. The molecular biology of coronaviruses. *Adv Virus Res*. 2006;66:193–292.
5. Mortola E, Roy P. Efficient assembly and release of SARS coronavirus-like particles by a heterologous expression system. *FEBS Lett*. 2004;576(1–2):174–178.
6. Mahase E. China coronavirus: WHO declares international emergency as death toll exceeds 200. *BMJ*. 2020;368:m408.
7. Worldometer. COVID-19 coronavirus pandemic. https://www.worldometers.info/coronavirus/. Last updated: June 21 2020. Accessed August 03 2020.
8. Kang S, Peng W, Zhu Y, et al. Recent progress in understanding 2019 novel coronavirus associated with human respiratory disease: detection, mechanism and treatment. *Int J Antimicrob Agents*. 2020;55(5):105950.
9. Wu C, Liu Y, Yang Y, Zhang P, Zhong W, Wang Y, Wang Q, Xu Y, Li M, Li X, Zheng M. Analysis of therapeutic targets for SARS-CoV-2 and discovery of potential drugs by computational methods. *Acta Pharm Sin B*. 2020;10(5):766–788.
10. Magrone T, Magrone M, Jirillo E. Focus on receptors for coronaviruses with special reference to angiotensin-converting enzyme 2 as a potential drug target-a perspective. *Endocr Metab Immune Disord Drug Targets*. 2020;20(6):807–811.
11. Jin Z, Du X, Xu Y, et al. Structure of M^{pro} from SARS-CoV-2 and discovery of its inhibitors. *Nature*. 2020;582(7811):289–293.
12. Zhang T, Wu Q, Zhang Z. Probable pangolin origin of SARS-CoV-2 associated with the COVID-19 outbreak. *Curr Biol*. 2020;30:1346–1351.
13. Bouchentouf S, Missoum N. Identification of compounds from *Nigella Sativa* as new potential inhibitors of 2019 novel coronasvirus (COVID-19): molecular docking study (published online April 01, 2020). *ChemRxiv*. 2020.
14. Suryawanshi SS, Patil RS, Jayannache PB, Palled MS, Alegaon SG. Screening and assessment of selected alkaloids as potential inhibitors of COVID-19 protease enzyme. *J Glob Trends Pharm Sci*. 2020;11:7711–7718.
15. Zhang DH, Wu KL, Zhang X, Deng SQ, Peng B. In silico screening of Chinese herbal medicines with the potential to directly inhibit 2019 novel coronavirus. *J Integr Med*. 2020;18(2):152–158.
16. Kumar D, Chandel V, Raj S, Rathi B. In silico identification of potent FDA approved drugs against coronavirus COVID-19 main protease: a drug repurposing approach. *Chem Biol Lett*. 2020;7:166–175.
17. Chandel V, Raj S, Rathi B, Kumar D. In silico identification of potent COVID-19 main protease inhibitors from FDA approved antiviral compounds and active phytochemicals through molecular docking: a drug repurposing approach (published online March 23, 2020). *Life Sci*. 2020.

18. Shah B, Modi P, Sagar SR. In silico studies on therapeutic agents for COVID-19: drug repurposing approach. *Life Sci*. 2020;252:117652.
19. Jassim SA, Naji MA. Novel antiviral agents: a medicinal plant perspective. *J Appl Microbiol*. 2003;95(3):412–427.
20. Flora of North America. Eastern purple coneflower, *Echinacea purpurea* (Linnaeus) Moench, Methodus. http://www.efloras.org/florataxon.aspx?flora_id=1&taxon_id=220004561. Accessed August 03 2020.
21. Foster S. *Echinacea: Nature's Immune Enhancer*. Rochester, Vermont: Healing Arts Press;1991.
22. A Vogel plant encyclopedia. *Echinacea purpurea* (L.) Moench purple coneflower. https://www.avogel.com/plant-encyclopaedia/echinacea_purpurea.php#:~:text=purpurea%20was%20listed%20in%20the,name%20%C2%ABMeyer's%20Blood%20Purifier%C2%BB. Accessed November 13 2020.
23. Flannery MA. From rudbeckia to echinacea: the emergence of the purple cone flower in modern therapeutics. *Pharm Hist*. 1999;41(2):52–59.
24. Melchart D, Linde K, Worku F, Bauer R, Wagner H. Immunomodulation with Echinacea-a systematic review of controlled clinical trials. *Phytomedicine*. 1994;1(3):245–254.
25. Thompson KD. Antiviral activity of Viracea against acyclovir susceptible and acyclovir resistant strains of herpes simplex virus. *Antiviral Res*. 1998;39:55–61.
26. Watanabe M. *Echinacea* (*Echinacea angustifolia* DC, *Echinacea pallida*, *Echinacea purpurea*). *Nat Stand Herb Suppl Ref*. 2007:118–130.
27. Merali S, Binns S, Paulin-Levasseur M, et al. Antifungal and anti-inflammatory activity of the genus. Echinacea. *Pharm Biol*. 2003;41(6):412–420.
28. Marriott B. An introduction to dietary supplements of plant origin. In: Maffei M, ed. *Dietary Supplements of Plant Origin*, New York: Taylor & Francis;2003:1–17.
29. Speroni E, Govoni P, Guizzardi S, Renzulli C, Guerra MC. Anti-inflammatory and cicatrizing activity of *Echinacea pallida* Nutt, root extract. *J Ethnopharmacol*. 2002;79(2):265–272.
30. Dalby-Brown L, Barsett H, Landbo AK, Meyer AS, Molgaard P. Synergistic antioxidative effects of alkamides, caffeic acid derivatives, and polysaccharide fractions from *Echinacea purpurea* on in vitro oxidation of human low-density lipoprotein. *J Agric Food Chem*. 2005;53(24):9413–9423.
31. Signer J, Jonsdottir HR, Albrich WC, Strasser M, Züst R, Ryter S. In vitro antiviral activity of Echinaforce®, an *Echinacea purpurea* preparation, against common cold coronavirus 229E and highly pathogenic MERS-CoV and SARS-CoV. *Virol J*. 2020;17(1):136.
32. Patil VS, Biradar PR, Attar V, Khanal P. In silico docking analysis of active biomolecules from *Cissus quadrangularis* L. against PPAR-γ. *Indian J Pharm Sci*. 2019;53:S332–S337.
33. Jarrahpour A, Fathi J, Mimouni M, et al. Petra, Osiris and Molinspiration (POM) together as a successful support in drug design: antibacterial activity and biopharmaceutical characterization of some azo Schiff bases. *Med Chem Res*. 2012;21:1984–1990.
34. Silva NS, Gonçalves LK, Duarte JL, et al. Computational analysis of physicochemical, pharmacokinetic, and toxicological properties of deoxyhypusine synthase inhibitors with antimalarial activity. *Comput Mol Biosci*. 2014;4(4):47–57.
35. Fadilah FA, Arsianti A, Kusmardi KU, Tedjo AR. Molecular docking studies of opened-chain analogues of antimycin A3 as caspases inhibitors of apoptosis in colorectal cancer. *Asian J Pharm Clin Res*. 2016;9(3):350–352.
36. UniProt Consortium. Reorganizing the protein space at the Universal Protein Resource (UniProt). *Nucleic Acids Res*. 2012;40:D71–D75.
37. Patil VS, Deshpande SH, Harish DR, et al. Gene set enrichment analysis, network pharmacology and in silico docking approach to understand the molecular mechanism of traditional medicines for the treatment of diabetes mellitus. *J Proteins Proteom*. 2020;11:297–310.
38. Khanal P, Patil BM. Gene set enrichment analysis of alpha-glucosidase inhibitors from *Ficus benghalensis*. *Asian Pac J Trop Biomed*. 2019;9(6):263–270.
39. Patil VS, Khatib NA. Triterpene saponins from *Barringtonia acutangula* (L.) Gaertn as a potent inhibitor of 11β-HSD1 for type 2 diabetes mellitus, obesity, and metabolic syndrome. *Clin Phytosci*. 2020;6:61.
40. Goyal B, Goyal D. Targeting the dimerization of main protease of coronaviruses: A potential broad-spectrum therapeutic strategy. *ACS Comb Sci*. 2020;22(6):297–305.
41. Wang GF, Shi LP, Ren YD, et al. Anti-hepatitis B virus activity of chlorogenic acid, quinic acid and caffeic acid in vivo and in vitro. *Antiviral Res*. 2009;83(2):186–190.
42. Khan MT, Ather A, Thompson KD, Gambari R. Extracts and molecules from medicinal plants against herpes simplex viruses. *Antiviral Res*. 2005;67(2):107–119.
43. Chiang LC, Chiang W, Chang MY, Ng LT, Lin CC. Antiviral activity of Plantago major extracts and related compounds in vitro. *Antiviral Res*. 2002;55(1):53–62.
44. Gamaleldin Elsadig Karar M, Matei MF, Jaiswal R, Illenberger S, Kuhnert N. Neuraminidase

inhibition of Dietary chlorogenic acids and derivatives-potential antivirals from dietary sources. *Food Funct*. 2016;7(4):2052–2059.
45. Tamura H, Akioka T, Ueno K, et al. Anti-human immunodeficiency virus activity of 3,4,5-tricaffeoylquinic acid in cultured cells of lettuce leaves. *Mol Nutr Food Res*. 2006;50(4–5):396–400.
46. Guo YJ, Luo T, Wu F, et al. Involvement of TLR2 and TLR9 in the anti-inflammatory effects of chlorogenic acid in HSV-1-infected microglia. *Life Sci*. 2015;127:12–18.
47. Ding Y, Cao Z, Cao L, Ding G, Wang Z, Xiao W. Antiviral activity of chlorogenic acid against influenza A (H1N1/H3N2) virus and its inhibition of neuraminidase. *Sci Rep*. 2017;7:45723.
48. Liu Z, Zhao J, Li W, et al. Computational screen and experimental validation of anti-influenza effects of quercetin and chlorogenic acid from traditional Chinese medicine. *Sci Rep*. 2016;6:19095.
49. Luo HJ, Wang JZ, Chen JF, Zou K. Docking study on chlorogenic acid as a potential H5N1 influenza A virus neuraminidase inhibitor. *Med Chem Res*. 2011;20:554–557.
50. Liu Z, Zhao J, Li W, et al. Molecular docking of potential inhibitors for influenza H7N9. *Comput Math Methods Med*. 2015;2015:480764.
51. Naghii MR. SARS-corona virus-2 origin and treatment, from coffee to coffee: a double-edged sword. *Int J Coron*. 2020;1:31–43.
52. Ding Y, Cao Z, Cao L, Ding G, Wang Z, Xiao W. Antiviral activity of chlorogenic acid against influenza A (H1N1/H3N2) virus and its inhibition of neuraminidase. *Sci Rep*. 2017;7:45723.